

## FORMATION OF THERMAL LOCALIZED STRUCTURES IN A WELD IN PULSE-ARC WELDING BY A NONMELTING ELECTRODE

O. N. Bezhin, V. A. Kosyakov, and R. A. Krektuleva

UDC 534.2

*The technological regimes of welding that promote uniform distribution of the properties over the length of a welded joint are studied by numerically modeling the formation of a weld seam by a nonmelting electrode.*

**Introduction.** The advent of program-controlled pulsed power sources has recently opened up fundamentally new possibilities in the development of the technologies of welding and welding-assisted deposition on the basis of a dosed energy supplied by an electrical arc according to a given algorithm.

It was found empirically [1, 2] that in definite pulse regimes, one can observe some positive phenomena during the formation of a single-piece joint. In particular, metal evaporation from a melt of a welded bath and the zone of thermal effect (ZTE) decreases, the defects in the welded joint become smaller in number, and the internal structure of the weld seam and the ZTE become more uniform. This contributes to the increase in the strength of the single-piece junction. It is assumed that these effects are attributed to the processes of self-arrangement of the substance [3, 4]. Knowledge of the reasons for and the basic features of the self-arrangement of the substance would allow one to design technological processes of welding that ensure the best operational characteristics of the welded joint. It is noteworthy that the pulse-arc technologies of welding are a complex object of the physical and mathematical modeling due to the great variety of the electromagnetic, thermal, chemical, mechanical, and other phenomena pertinent to the technological cycle. In view of this, it is of interest to develop and study some of the basic mathematical models of the pulse-arc welding processes, which most affect the final properties of the welded joint. One of them is the interaction between the electrical arc (as a source of the concentrated thermal energy) and the object to be welded, because the energy supply determines the width and depth of the melted zone, the ZTE dimensions, and the crystallization and the recrystallization in the weld seam and the near-seam zone, which in turn determine the internal micro- and mesostructure.

In this work, we numerically solve the spatial dynamic problem of the heat conduction in the pulse heat supply from a moving source of heating (the arc). The effect of the frequency of pulses and the rate of welding on the formation of the thermal pattern in the junction of two steel plates of finite sizes is studied.

**Formulation of the Problem.** Generally, the system of equations which describes the interaction between the electrical arc and the butt-weld plates includes the following equations:

- The spatial heat-conduction equation

$$C(T)\rho(T) \frac{\partial T}{\partial t} = \operatorname{div} [\lambda(T) \operatorname{grad} T] + Q \quad (1)$$

with the boundary conditions

$$-\lambda(T) \frac{\partial T}{\partial n} = \alpha(T)(T - T_0) \quad (2)$$

---

Institute of Physics of Strength and Materials Science, Siberian Division, Russian Academy of Sciences, Tomsk 634021. Translated from *Prikladnaya Mekhanika i Tekhnicheskaya Fizika*, Vol. 39, No. 6, pp. 172–177, November–December, 1998. Original article submitted January 8, 1997; revision submitted March 17, 1997.

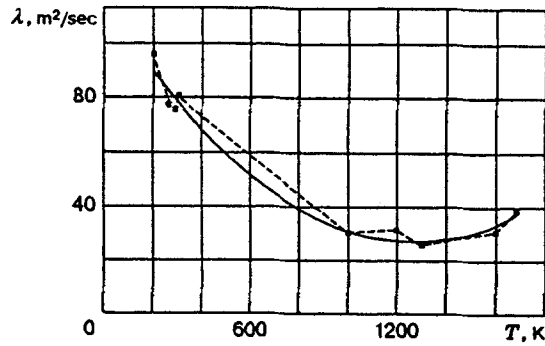


Fig. 1

on the surface (except for the region of action of the arc) and

$$\lambda(T) \frac{\partial T}{\partial n} = Q \quad (3)$$

in the zone of action of the arc;

- The equation of motion of the melting or crystallization front (the Stefan condition)

$$LV_c = \lambda_{\text{solid}} \frac{\partial T}{\partial n} - \lambda_{\text{liquid}} \frac{\partial T}{\partial n}; \quad (4)$$

- The equation of a heat flux from the arc (the equations of the normal distribution [5])

$$Q = \eta IU(k/\pi) \exp(-kr^2). \quad (5)$$

The following notation is introduced in Eqs. (1)–(5):  $T$  is the current temperature,  $T_0$  is the ambient temperature;  $C(T)$ ,  $\rho(T)$ , and  $\lambda(T)$  are the functional dependences of the heat capacity, the density, and the heat conduction on the temperature,  $\alpha(T)$  is the coefficient of heat exchange with the ambient medium,  $\mathbf{n}$  is the normal vector to the surface,  $L$  is the specific heat of the phase transition,  $V_c$  is the velocity of the melting (crystallization) front;  $\lambda_{\text{solid}}$  and  $\lambda_{\text{liquid}}$  are the heat conduction of the solid and liquid phases during the phase transition;  $I(t)$  is the current,  $U(t)$  is the voltage,  $\eta$  is the efficiency of the arc,  $k$  is the coefficient of concentration of the flux,  $r$  is the radius of the active spot of the heated surface,  $t$  is the time; and  $x$ ,  $y$ , and  $z$  are the spatial coordinates.

Problem (1)–(5) is solved numerically by the finite-difference method [6]. Each plate to be welded is  $80 \times 20 \times 8$  mm in dimension. Since the plates are symmetrical relative to the source of heating, the problem is solved only for one plate with a  $80 \times 20 \times 8$  calculation grid. We employ the algorithm of partition of the three-dimensional problem into two two-dimensional problems as in [7]. In addition, the solution of the thermal problem takes into account the nonlinear character of the thermophysical properties  $C(T)$ ,  $\lambda(T)$ , and  $\rho(T)$ . The experimental data for St. 45 steels from [8, 9] are approximated by a polynomial of the form  $\sum_{i=0}^n a_i T^i$ , the number of terms in which is determined by the standard procedures for solving the regression problem [10].

Figure 1 illustrates the "smoothing" of the heat conductivity  $\lambda(T)$  by a function of the form  $\lambda(T) = 112.33637 - 0.12759 T + 0.00005 T^2$  (the solid and dashed curves refer to the calculated and experimental data, respectively).

The other parameters are approximated similarly. We failed to find reliable data on the variation of the thermal and physical parameters for this steel make at temperatures higher than the melting point  $T_{\text{melt}}$  and, therefore, for  $T > T_{\text{melt}}$  we use the approximating dependences constructed using the experimental data for the lower temperature region ( $T < T_{\text{melt}}$ ). For the same reason, we assume that  $\lambda_{\text{solid}} = \lambda_{\text{liquid}}$  at the melting point; this permits us not to include the Stefan condition explicitly. The arc parameters  $r$ ,  $\eta$ , and  $k$  are set as in [5].

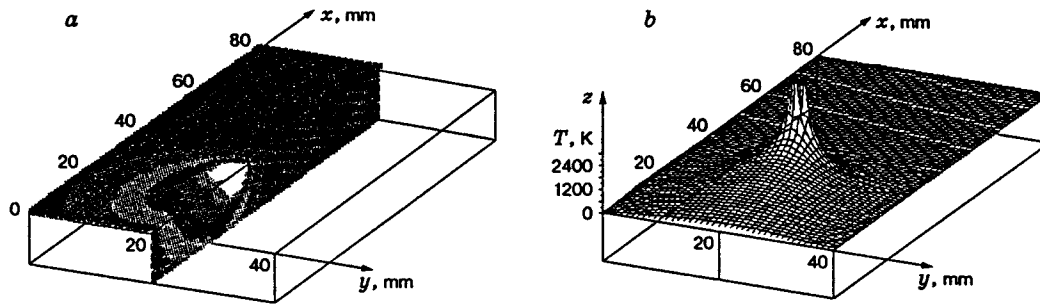


Fig. 2

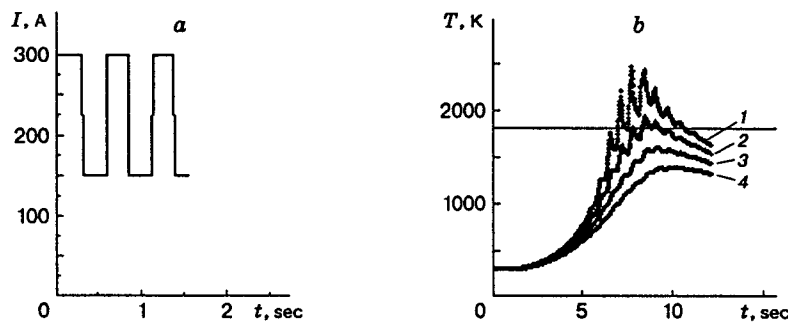


Fig. 3

In the numerical experiment, we considered the technological regimes used in welding practice in argon. For example, the rate of welding was varied from 0.001 to 0.004 m/sec; the volt-ampere characteristics (VAC) differed by no more than 20%: the pulse current was  $I_{\text{pulse}} = 350$ , the current in the pause was  $I_{\text{pause}} = 150$ , and the pulse voltage was  $U_{\text{pulse}} = 52$  and the voltage in the pause was  $U_{\text{pause}} = 12$  V. The frequency and shape of the pulses were not restricted.

**Discussion of Calculation Results.** We analyze the solution of the thermal problem (1)–(5). Figure 2 shows the temperature distribution in a welded joint at the rate of welding  $V_{\text{weld}} = 0.002$  m/sec, the rectangular shape of the pulse ( $t_{\text{pulse}} = t_{\text{pause}} = 0.3$  sec), and the basic values of the VAC indicated above. The butt-jointing is denoted by the vertical cut in Fig. 2a. The thermal fields generated in 24 sec are shown in Fig. 2a in the cross section and on the surface. The regions with different temperatures are hatched. Reckoning is performed from the internal (unhatched) region, i.e., the zone of metal melting wherein the material reaches the boiling point; at the boundary of this zone the temperature is equal to the melting point ( $T_{\text{melt}} = 1808$  K). Inside each subsequent region, the temperature falls off by 500 deg from boundary to boundary.

Figure 2b shows the temperature distribution in the near-surface layer at a depth of 1 mm. It is noteworthy that the thermal-wave front is localized in the narrow region. This is due to the nonlinearity of the heat-conducting properties of the medium (the thermal conductivity, the diffusivity, and the coefficient of heat transfer with the ambient medium within 300–1800 K for St. 45 change three to fourfold [8, 9]), the continuous displacement of the source of heating with a certain velocity, and the pulse character of the heat supply.

The numerical experiments performed in various regimes of welding showed that the thermal structures can have a complex time-varying configuration. We also separated a certain set of elementary topological forms or eigenfunctions (according to the terminology of [11]) which are involved in the complex thermal structures. For illustration, we analyze the heat transfer in a regime of low-frequency modulation of the welding current (less than 10 Hz). In this regime, the material “tunes” into the frequency of oscillations of the heat flux  $Q$  so that the frequency of temperature oscillations of the material becomes synchronous with the frequency of

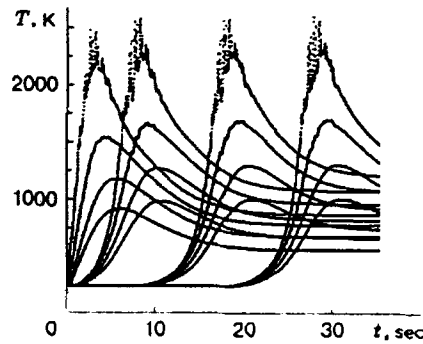


Fig. 4

thermal pulses not only in the arc-spot area but also in its neighborhood. Figure 3 shows the shape of the welding-current pulses (Fig. 3a) and the temperature variation in time at the points which are coaxial with the center of the arc spot and are located at a depth of 2, 3, 4, and 5 mm, respectively (curves 1-4 in Fig. 3b).

The calculations also showed that, in practice, the thermal vibration in the weld seam is not affected by the geometry of the rectangular, sinusoidal, etc. pulses. At the same time, the larger the oscillation period, the more strikingly the components of the thermal structures show up. For low-frequency power supply, one can distinguish four characteristic types of elementary structures formed in the following sequence:

- (a) in the transition from pause to pulse,
- (b) in the pulse,
- (c) in the transition from pulse to pause,
- (d) in the pause.

This sequence was observed in each phase. However, the maximum temperature amplitude for each characteristic increased with the number of phases, since the rate of welding was lower than the rate of heat supply. This enlarges the zone of alloying of the welded seam and the ZTE, which changes the thermophysical properties and usually deteriorates the strength and operational characteristics of the weld seam. In practice, the thermomechanical properties are "equalized" by thermal cycling [2].

These features made it possible to attempt to select a technological regime which forces the material to self-arrange during the intense thermal action. The calculations showed that the high stability of the temperature regimes can be attained by regulating the frequency of energy pulses and the rate of welding. If necessary, the control parameters can be supplemented by other technical characteristics ( $t_{\text{pulse}}$ ,  $t_{\text{pause}}$ , etc.). Figure 4 illustrates the thermal structures formed in the zone of seam alloying as the rate of welding increases ( $V_{\text{weld}} = 0.002 + 0.0005t$ ) and for the pulse with a period of 0.6 sec ( $t_{\text{pulse}} = t_{\text{pause}} = 0.3$  sec). The diagram shows the curves for the points having the following coordinates (in millimeters): [(10,1), (10,2), (10,4), (10,6)], [(20,1), (20,2), (20,4), (20,6)], [(40,1), (40,2), (40,4), (40,6)], and [(60,1), (60,2), (60,4), (60,6)]. The square brackets indicate the equidistant points from the left edge of the plate. The first figure in parentheses indicates this distance, and the second figure refers to the depth.

It is easy to note that the four groups of curves are similar. The character of the temperature variation at various points of space is identical within the localization regions. Stable thermal oscillations in the region of increased temperatures during welding are ensured by the conditions of thermal cycling, which improves the efficiency of the welding technology.

**Conclusions.** (1) The calculational model of one of the basic stages of the technological process of welding, namely, the stage of thermal interaction between the welding arc and the product being welded, has been given. The model adequately reflects the real process: it takes into account the spatial geometry of the welded parts, the nonlinear properties of the thermophysical characteristics, and the possibility of pulse heat supply at a variable rate of welding.

(2) The solution of the thermal problem has allowed us to show the effectiveness of the pulse conditions of welding at low-frequency currents (less than 10 Hz), because this offered the possibility of creating stable thermal structures during welding along the entire weld seam, which ensures homogeneous thermomechanical properties in the seam and the ZTE and, hence, the high quality of this seam.

The calculation results can be used in actual technological processes.

## REFERENCES

1. F. A. Vagner, *Equipment and Techniques of Welding by a Pulsating Arc* [in Russian], Energiya, Moscow (1989).
2. I. Grivnyak, *Weldability of Steels* [Russian translation], Mashinostroenie, Moscow (1984).
3. I. V. Zuev, "Self-arrangement (synergetics) of welding and soldering. Work of seam formation," *Svarochn. Proizv.*, No. 9, 13–16 (1995).
4. R. I. Zainetdinov and S. N. Kiselev, "Deformation and fracture of welded structures from the viewpoint of synergetics and the theory of Markov processes," *Svarochn. Proizv.*, No. 3, 16–19 (1995).
5. V. A. Sudnik and A. S. Rybakov, "Calculational-experimental models of the moving arc of a nonmelting electrode in argon," *Svarochn. Proizv.*, No. 11, 32–34 (1990).
6. A. A. Samarskii, *Theory of Difference Schemes* [in Russian], Nauka, Moscow (1983).
7. A. V. Panyukhin and B. N. Bad'yanov, "Mathematical model of melting in laser microwelding of heterogeneous materials," *Svarochn. Proizv.*, No. 8, 8–9 (1993).
8. I. S. Grigor'ev and E. Z. Meilikhov (eds.), *Physical Quantities: Handbook* [in Russian], Energoatomizdat, Moscow (1991).
9. A. A. Shmychkov, *Handbook of the Thermist* [in Russian], Mashgiz, Moscow (1956).
10. S. L. Akhnazarova and V. V. Kafarov, *Methods of Optimizing the Experiment in Chemical Technology* [in Russian], Vysshaya Shkola, Moscow (1985).
11. A. A. Samarskii, V. A. Galaktionov, S. P. Kurdyumov, and A. P. Mikhailov, *Peaking Regimes in Problems for the Quasi-Linear Parabolic Equations* [in Russian], Nauka, Moscow (1987).